*Vietnam Journal of Science and Technology* ***56*** *(1A) (2018) 93-101*

# X-RAY PHOTOELECTRON SPECTROSCOPIC STUDY ON HIGH-ELECTRON-MOBILITY GALLIUM AND HYDROGEN CO-DOPED ZINC OXIDE THIN FILMS

**Anh Thanh Tuan Pham[1, *], Dung Van Hoang[1], Truong Huu Nguyen[1], Nguyen Bao Thu Le[2], Thang Bach Phan[1, 3], Vinh Cao Tran[1]**

[1]*Laboratory of Advanced Materials, University of Science, Vietnam National University, Ho Chi Minh City, Viet Nam*

[2]*Department of Mathematics and Physics, University of Information Technology, Vietnam National University, Ho Chi Minh City, Viet Nam*

[3]*Center for Innovative Materials and Architectures, Vietnam National University, Ho Chi Minh City, Viet Nam*

[*] Email: *pttanh@hcmus.edu.vn*

Received: 15 August 2017; Accepted for publication: 5 February 2018

## ABSTRACT

In this study, gallium and hydrogen co-doped ZnO (HGZO) thin films were investigated. The films were deposited by sputtering from Ga-doped ZnO (GZO) ceramic target in hydrogen and argon plasma. The as-deposited HGZO films possess enhanced electron mobility of 48.6 $cm^2$/Vs as compared to that of 39.4 $cm^2$/Vs of GZO films, sputtered from the same target. Because of insignificant variation in crystallinity, this improvement is attributed to roles of hydrogen in crystalline lattice structure of the films. X-ray photoelectron spectroscopy (XPS) is employed as an essential technique for quantitative analyses and chemical binding states of films constituent elements. The roles of hydrogen are clarified through the binding states of Zn 2p, O 1s and Ga 3d. Obtained results suggest that the films are deposited more effectively in hydrogen plasma. Some point defects such as oxygen vacancies ($V_O$), dangling bonds can be passivated in form of $H+V_O \rightarrow H_O$ and O–H bonds. As a result, the reduction of scattering centers is indicated as a reason for the mobility improvement of the HGZO films.

*Keywords:* ZnO thin films, high electron mobility, XPS, chemical binding states, passivation.

## 1. INTRODUCTION

Over the past years, Ga-doped ZnO (GZO) thin films as a class of transparent conducting oxide (TCO) have attracted much attention in the world. It is proved to be a potential replacement for Sn-doped $In_2O_3$ (ITO) in photovoltaic and optoelectronic devices [1, 2]. The nature of interesting characteristics of GZO films comes from the bonding distance with O (1.92 Å) and ionic radius (0.62 Å) of Ga are similar to those of Zn (1.97 Å and 0.74 Å), respectively [3]. This facilitates the $Zn^{2+}$ substitution of $Ga^{3+}$ and reduces structural lattice distortion. By selecting a reasonable doping ratio, the GZO films can achieve the order of $10^{-4}$ Ωcm in

resistivity and more than 80 % in visible light transmittance as reported in some papers [4–7]. In these papers, however, the low resistivity is mainly contributed by high carrier concentration (~$10^{21}$ $cm^{-3}$). This induces decreased transmittance in the near-IR region due to free-carrier absorption. Consequently, high electron mobility is more effective than high carrier concentration in expanding high transmittance from the visible to near-IR regions and reducing resistivity.

Hydrogen (H) capability in improving electron mobility in ZnO-based films such as H-doped ZnO (HZO), H and Al co-doped ZnO (HAZO) has been reported [8, 9]. Also, the combination of H and Ga dopants in ZnO (HGZO) films is expected to produce better optoelectronic properties than HZO and HAZO films. A large number of studies on H-related ZnO films have been carried out to understand roles of hydrogen. The presence of hydrogen and its impacts on films are displayed via analytic techniques, such as X-ray diffraction (XRD) [8, 10, 11]; morphology analysis [12–14], secondary ion mass spectroscopy (SIMS) [8, 15]; Fourier transform infrared (FT-IR) [16–18]; Raman spectroscopy [16, 19]. In literature, however, X-ray photoelectron spectroscopy (XPS), a strong and effective technique to provide information of chemical binding states, has been limitedly used to demonstrate the roles of hydrogen in HGZO films, especially in characterization of high electron mobility.

In this work, therefore, a comparison of electrical properties of GZO films deposited in hydrogen and argon plasma with those prepared in pure Ar is carried out. In which, the feature of high electron mobility of HGZO films is emphasized. The XPS technique for studying contribution of hydrogen in this feature of HGZO films is also discussed.

## 2. MATERIALS AND METHODS

The home-made GZO sputtering target containing 0.5 wt.% $Ga_2O_3$ and 99.5 wt.% ZnO (99.99 % all in purity, Merck, Germany) was fabricated by high-temperature sintering method. The target was employed to deposit GZO thin films on glass substrate in pure Ar ambient by DC magnetron sputtering (Leybold UNIVEX 450). To prepare HGZO thin films, small amount of hydrogen gas was introduced into sputtering atmosphere while other deposition parameters were constant. The substrate temperature and sputtering power were maintained at 200$^{o}$C and 60 W, respectively, during deposition.

The films were checked by using a Stylus profilometer (Veeco DEKTAK 6M) to determine thickness (~1300 nm). To clarify the role of hydrogen in HGZO films, composition ratios and chemical binding states of Zn, O and Ga elements were analyzed by X-ray photoelectron spectroscopy (XPS, Thermo Scientific ESCALAB 250, at the Instrumentation Center – National Taiwan University) with Al $K_\alpha$ (1486.6 eV) radiation as X-ray source. The carrier concentration, mobility and resistivity of the films were obtained from Hall effect-based measurement (Ecopia HMS 3000). A X-ray diffraction system (XRD, Bruker D8 ADVANCE) was used to verify crystalline structure of the films.

## 3. RESULTS AND DISCUSSION

### 3.1. Electrical characterization

The typical electrical parameters of GZO and HGZO thin films determined from Hall measurement at room temperature are summarized in Table 1. The HGZO films ($5.6\times10^{-4}$ Ωcm)

have lower resistivity as compared to GZO films ($10.6\times10^{-4}$ Ωcm). It is evidently due to both carrier concentration and mobility.

*Table 1.* Carrier concentration (n), mobility (μ), resistivity (ρ) and sheet resistance ($R_S$) of GZO and HGZO thin films.

| Thin films | n ($\times10^{20}$ cm$^{-3}$) | μ (cm$^2$/Vs) | ρ ($\times10^{-4}$ Ωcm) | $R_S$ (Ω/sq.) |
|---|---|---|---|---|
| **GZO** | 1.5 | 39.0 | 10.6 | 7.5 |
| **HGZO** | 2.3 | 48.6 | 5.6 | 4.2 |

Firstly, the carrier concentration of HGZO films ($2.3\times10^{20}$ cm$^{-3}$) is higher than that of GZO films ($1.5\times10^{20}$ cm$^{-3}$). It suggests hydrogen as a source contributing electrons for conduction. This is good agreement with formation capability of hydrogen shallow donor states (~0.03 – 0.1 eV under conduction band) [20, 21]. It is well-known that free electrons in n-type TCO films come from intrinsic and extrinsic sources. Normally, the former including native defects ($Zn_i$, $V_{Zn}$, $O_i$, $V_O$, …) provides carrier concentration in order of $10^{18}$ cm$^{-3}$ corresponding to resistivity in order of $10^{-3}$ Ωcm in pure ZnO films. In this work, the latter consist of defects relating to hydrogen and gallium. Among them, hydrogen donors only induce the minimum resistivity in order of $10^{-2}$ Ωcm [22]. Thus, electrons are not only from the intrinsic and hydrogen donors, but also come from another source (gallium donors). Although using the same sputtering target, the gallium ratio in GZO and HGZO films may be different. This will be discussed in detail below.

Secondly, the mobility of HGZO films is 48.6 cm$^2$/Vs that is higher than that of GZO films (39 cm$^2$/Vs) by 25 %. It is well-known that electron mobility in n-type TCO films depends on the scattering mechanisms mainly induced by lattice vibration, grain boundaries and defects. Because the obtained films have carrier concentration in order of $10^{20}$ cm$^{-3}$ which is much higher than that ($10^{16}$ cm$^{-3}$) of ZnO single crystals [23], the phonon scattering is not significant. Besides, the carrier concentration of the highly degenerated GZO and HGZO films is also higher than $10^{18}$ cm$^{-3}$, so the grain boundary scattering is not dominant [8]. Thus, the remaining dominant mechanism is ionized impurities scattering which can be strongly influenced by hydrogen. Typically, hydrogen passivation can decrease dangling bonds, electron traps and defects in ZnO-based films [10, 13, 16, 24]. This results in reduction of scattering centers and enhancing the mobility. However, it is necessary to consider more analyses for how hydrogen passivates defects in the HGZO films.

### 3.2. Crystalline structure

*Table 2.* Crystallographic information of GZO and HGZO thin films.

| Thin films | 2θ position (deg.) | FWHM (deg.) | Average crystal size (nm) |
|---|---|---|---|
| **GZO** | 34.47 | 0.2033 | ~40 |
| **HGZO** | 34.41 | 0.2570 | ~30 |

To examine the presence of hydrogen and its effects on crystallization of the films, XRD spectroscopy was taken at room temperature and displayed in Figure 1.

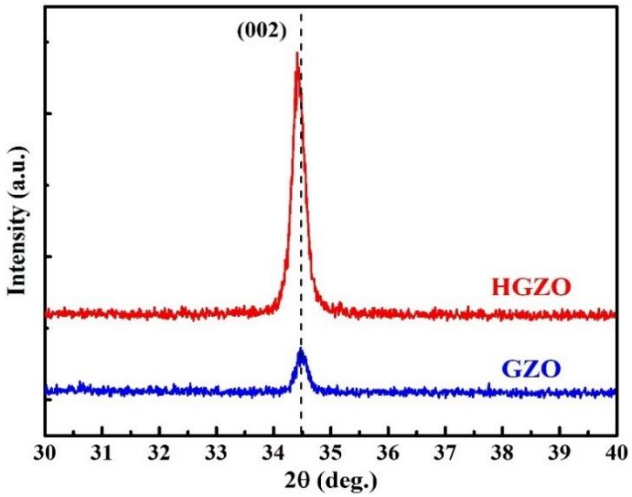


*Figure 1.* XRD patterns of GZO and HGZO thin films.

Figure 1 shows the hexagonal wurtzite-structural characterization of ZnO-based films with (002) plane-oriented growth along c-axis and perpendicular to the substrate. No additional peaks relating to gallium and hydrogen phases are observed. From the XRD spectra, the typically crystallographic parameters of the films are listed in Table 2.

It is seen that the 2θ-position of (002) peak of HGZO films (34.41$^{o}$) is smaller than that of GZO films (34.47$^{o}$). This suggests the insertion of hydrogen into bond-centered sites of Zn–O and/or Ga–O. The similar results were also reported in the literature [8, 10, 16]. Besides, the FWHM increases with hydrogen introduction. Large FWHM means the reduction of crystallite dimension [8]. Average crystal size of HGZO films is ~30 nm, smaller than that of GZO films (~40 nm), which are estimated by using Debye-Scherrer's formula. Although the HGZO films possess small average crystal size, their (002)-peak diffraction intensity are very high as compared to that of GZO films. It suggests a better intra-crystalline quality (inside grains) of HGZO films with less traps and scattering centers than that of GZO films, which results in high mobility.

### 3.3. X-ray photoelectron analysis

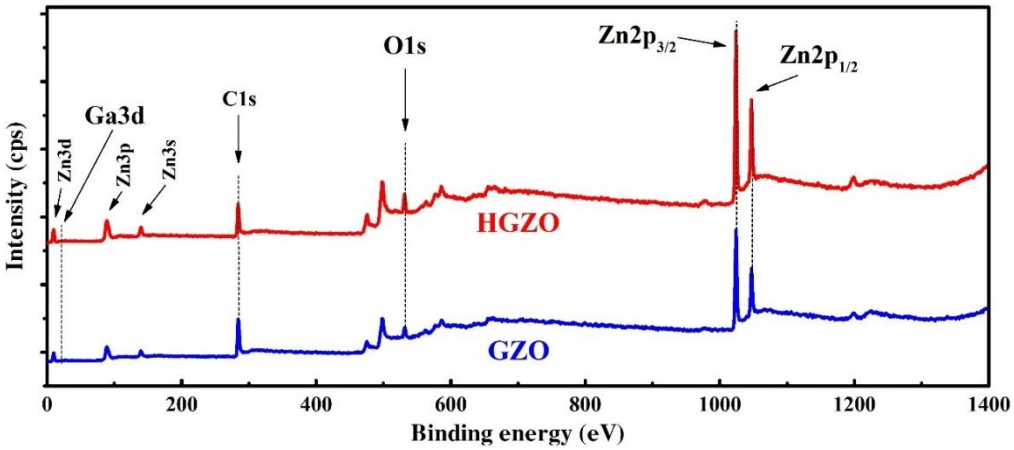


*Figure 2.* XPS survey spectra of GZO and HGZO films.

As mentioned above, the differences in the properties between the GZO and HGZO films can be induced by hydrogen. For further information, the composition and chemical binding states of constituent elements in the films were determined by XPS spectra, as shown in Figure 2.

The positions of all peaks in the XPS spectra are aligned with C 1s state (284.4 eV). Note that hydrogen cannot be identified by XPS method due to the small size and simple electronic configuration of hydrogen atom [25]. The hydrogen contribution is therefore considered through binding states of other elements, such as Zn 2p, Ga 3d and O 1s.

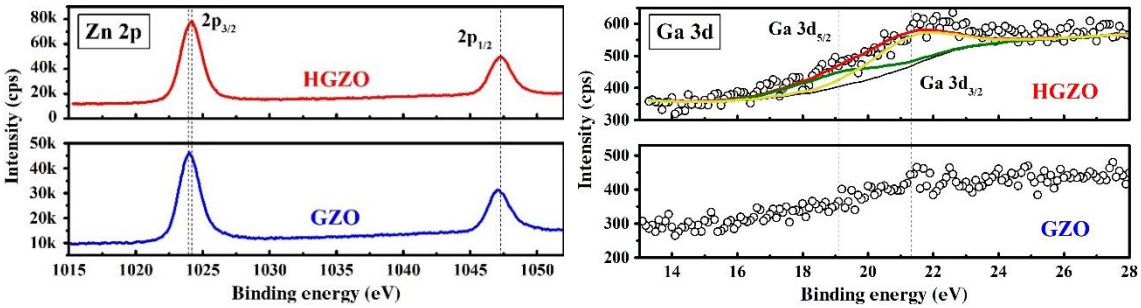


*Figure 3.* XPS spectra of Zn 2p and Ga 3d core-level states of GZO and HGZO films.

Figure 3 exhibits the XPS spectra of Zn 2p and Ga 3d core-level states with double peak characterization of GZO and HGZO thin films. For the Zn 2p state, the GZO films show two peaks located at 1024 eV (Zn $2p_{3/2}$) and 1047 eV (Zn $2p_{1/2}$). The energy separation is 23 eV for ZnO-based films, which is in line with the other reports [26, 27]. However, there is a small variation in binding energy of Zn 2p states of HGZO films. Correspondingly, the peaks situate at 1024.2 eV and 1047.2 eV, which means a 0.2 eV shift toward higher binding energy as compared to GZO films. It can be attributed to the presence of Zn-H bonds in HGZO films [8]. For the Ga 3d state, it cannot be observed in GZO films, which may be due to the very small Ga content in the films. On the other hand, the broad Ga 3d peak can be deconvoluted into two sub-peaks which are assigned to the Ga $3d_{5/2}$ and Ga $3d_{3/2}$ states, respectively by using Gauss-Lorentz mixed function [28]. The evolution of Ga 3d peaks suggests the significant increase of Ga content in the HGZO films which is estimated in Table 3.

*Table 3.* The Ga 3d core-level data of GZO and HGZO films.

| Thin films | States | Binding energy (eV) | FWHM (eV) | Atomic ratios (at.%) |
|---|---|---|---|---|
| **GZO** | – | – | – | Very small |
| **HGZO** | Ga $3d_{5/2}$ | 19.1 | 2.95 | 2.68 ± 0.01 |
| | Ga $3d_{3/2}$ | 21.3 | 2.63 | |

It is seen that the XPS Ga 3d peak of HGZO films is overlapped by two components located at 19.1 eV (Ga $3d_{5/2}$) and 21.3 eV (Ga $3d_{3/2}$). It indicates that Ga ions exist with the valence of +3 in the films. The ratio of Ga content also increases in HGZO films as compared to GZO films. This suggests more effective film-deposition in the hydrogen plasma. *Akazawa*

reported that a $Ga^{3+}$ and a $H^+$ ions can replace two $Zn^{2+}$ ions easily to maintain charge neutrality [22]. Thus, hydrogen is believed as a factor which facilitates $Ga^{3+}$ to substitute $Zn^{2+}$ sites in the films.

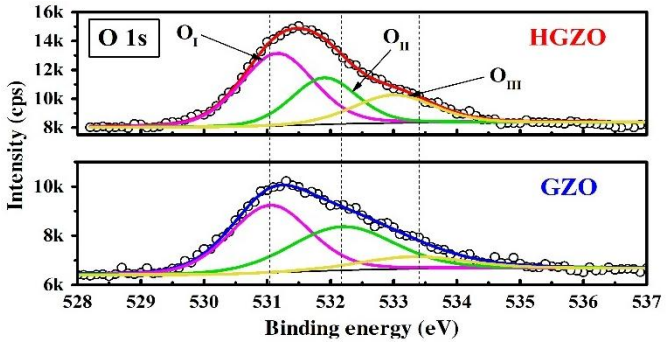


*Figure 4.* XPS spectra of O 1s core-level state and its deconvolution of GZO and HGZO films.

Figure 4 illustrates XPS spectra of O 1s core-level states of GZO and HGZO thin films. It is clearly seen that the shape of O 1s peaks is asymmetric. Similarly to the Ga 3d state, the peaks of O 1s state are deconvoluted into three components which situate at ~531 eV, ~532 eV and ~533 eV (notate as $O_I$, $O_{II}$ and $O_{III}$ respectively). It is well suitable with the analyses of O 1s state in the other studies of ZnO-based films [26, 29]. Among them, the $O_I$ and $O_{II}$ peaks relate to $O^{2-}$ ionic bonds. The $O_I$ characterizes for the $O^{2-}$ binding at lattice points of hexagonal-wurtzite ZnO, whereas $O_{II}$ are in oxygen-deficient regions (oxygen vacancies – $V_O$). The $O_{III}$ with the highest energy is referred to $Zn^{2+}$ binding to hydroxyl group (–OH). The variation in intensity of these components is evaluated through relative intensity ratios as shown in Table 4.

*Table 4.* The O 1s core-level data of GZO and HGZO films.

| Thin films | Binding energy (eV) | | | Relative intensity ratio | |
|---|---|---|---|---|---|
| | $O_I$ | $O_{II}$ | $O_{III}$ | $O_{II}$ / $O_I$ | $O_{III}$ / $O_I$ |
| **GZO** | 531.1 | 532.2 | 533.3 | 0.91 | 0.77 |
| **HGZO** | 531.2 | 531.9 | 533.0 | 0.87 | 0.79 |

The variation of ratio $O_{II}/O_I$ is considered as a result of the modification of $V_O$ concentration in the films. The ratio decreases from 0.91 (GZO) to 0.87 (HGZO), which means the reduction of $V_O$ concentration with hydrogen introduction. It can be explained by hydrogen trapped at $V_O$ sites as defect formation reaction: $H^+ + V_O \longrightarrow H_O^+$ [8], where $H_O$ is substitutional hydrogen and also contributes electron to conduction band. Besides, the ratio $O_{III}/O_I$ increases from 0.77 (GZO) to 0.79 (HGZO), which means the increase of –OH group attached to the cations (Zn, Ga).

Consequently, the above XPS analyses show the evidences of defects variation in the HGZO films. The analysis of Ga 3d state shows the better deposition of HGZO films than GZO films due to hydrogen plasma. This enhances substituted $Ga^{3+}$ and reduces probability of interstitial $Ga^{3+}$. The analysis of O 1s state indicates the decrease of $V_O$-related defects. Furthermore, the increase of –OH and –H binding to Zn (and/or Ga) suggests the passivation of dangling bonds in the films and on the film's surface, which are interpreted from the Zn 2p and

O 1s states. All these things reduce the scattering centers, improve intra-crystalline quality, which leads to enhance electron mobility in the HGZO films.

## 4. CONCLUSIONS

In this study, the gallium and hydrogen co-doped ZnO (HGZO) thin films were fabricated successfully by using DC magnetron sputtering method. The films obtain high electron mobility of 48.6 $cm^2/Vs$, which is due to intra-crystallinity improvement. It is attributed to the reduction of scattering centers, which is suggested by the XRD, especially XPS techniques. Through the XPS analyses, some roles of hydrogen in improving mobility can be realized, such as: (i) increasing substituted $Ga^{3+}$ in the films by the charge neutral mechanism, (ii) reducing $V_O$-related defects by capturing $H^+$ to form the $H_O$ donor, and (iii) passivating dangling bonds by creating the –OH bonds. However, it is still necessary to carry out further studies for more evidences.

***Acknowledgements.*** The research funding from Vietnam National University – Ho Chi Minh City (VNU-HCM) (Grant number: B2017-18-09) was acknowledged. The authors also acknowledge Prof. Kuei-Hsien Chen and Dr. Deniz P. Wong (IAMS, Academia Sinica, Taiwan) for support of XPS measurement.

## REFERENCES

1. Liu Y., Li Y., and Zeng H. - ZnO-based transparent conductive thin films: doping, performance, and processing, J. Nanomater. **2013** (2013) 196521.
2. Mccluskey M. D. and Jokela S. J. - Defects in ZnO, J. Appl. Phys. **106** (2009) 071101.
3. Liu J., Zhang W., Song D., Ma Q., and Zhang L. - Gallium-doped zinc oxide targets fabricated by sintering: Impact of target quality on sputtered thin film properties, Mater. Sci. Semicond. Process. **27** (2014) 1–11.
4. Makino H., Sato Y., Yamamoto N., and Yamamoto T. - Changes in electrical and optical properties of polycrystalline Ga-doped ZnO thin films due to thermal desorption of zinc, Thin Solid Films **520** (2011) 1407–1410.
5. Ko Y., Kim K., and Kim Y. - Effects of substrate temperature on the Ga-doped ZnO films as an anode material of organic light emitting diodes, Superlattices Microstruct. **51** (2012) 933–941.
6. Moditswe C., Muiva C. M., and Juma A. - Highly conductive and transparent Ga-doped ZnO thin films deposited by chemical spray pyrolysis, Opt. - Int. J. Light Electron Opt. **127** (2016) 8317–8325.
7. Fortunato E., Raniero L., Silva L., Goncalves A., Pimentel A., Barquinha P., Águas H., Pereira L., Goncalves G., Ferreira I., Elangovan E., and Martins R. - Highly stable transparent and conducting gallium-doped zinc oxide thin films for photovoltaic applications, Sol. Energy Mater. Sol. Cells **92** (2008) 1605–1610.
8. Gaspar D., Pereira L., Gehrke K., Galler B., Fortunato E., and Martins R. - High mobility hydrogenated zinc oxide thin films, Sol. Energy Mater. Sol. Cells **163** (2017) 255–262.
9. Calnan S., and Tiwari A. N. - High mobility transparent conducting oxides for thin film solar cells, Thin Solid Films **518** (2010) 1839–1849.

10. Huang C. C., Wang F. H,, and Yang C. F. - Effects of deposition temperature and hydrogen flow rate on the properties of the Al-doped ZnO thin films and amorphous silicon thin-film solar cells, Appl. Phys. A **112** (2013) 877–883.
11. Li M. C., Kuo C. C., Peng S. H., Chen S. H., and Lee C. C. - Influence of hydrogen on the properties of Al and Ga-doped ZnO films at room temperature, Appl. Opt. **50** (2011) C197.
12. Tark S. J., Kang M. G., Park S., Lee S. H., Son C. S., Lee J. C., and Kim D. - Characterization of hydrogenated Al-doped ZnO films prepared by multi-step texturing for photovoltaic applications, Curr. Appl. Phys. **11** (2011) 362–367.
13. Wang F., Chen X., Geng X., Zhang D., Wei C., Huang Q., Zhang X., and Zhao Y. - Development of natively textured surface hydrogenated Ga-doped ZnO-TCO thin films for solar cells via magnetron sputtering, Appl. Surf. Sci. **258** (2012) 9005–9010.
14. Huang C., Wang M., Deng Z., Cao Y., Liu Q., Huang Z., Liu Y., Guo W., and Huang Q. - Effects of hydrogen annealing on the structural, optical and electrical properties of indium-doped zinc oxide films, J. Mater. Sci. Mater. Electron. **21** (2010) 1221–1227.
15. Takeda S., and Fukawa M. - Characteristic of hydrogenated Ga-doped ZnO films grown by DC magnetron sputtering using $H_2$/Ar gas, MRS Proc. **813** (2004) H3.5.
16. Park Y. R., Kim J., and Kim Y. S. - Effect of hydrogen doping in ZnO thin films by pulsed DC magnetron sputtering, Appl. Surf. Sci. **255** (2009) 9010–9014.
17. Lavrov E. V., Weber J., Börrnert F., Van de Walle C. G., and Helbig R. - Hydrogen-related defects in ZnO studied by infrared absorption spectroscopy, Phys. Rev. B **66** (2002) 165205.
18. Lavrov E. V., Börrnert F., and Weber J. - Dominant hydrogen-oxygen complex in hydrothermally grown ZnO, Phys. Rev. B **71** (2005) 1–6.
19. Koch S. G., Lavrov E. V., and Weber J. - Interplay between interstitial and substitutional hydrogen donors in ZnO, Phys. Rev. B **89** (2014) 1–8.
20. Gallino F., Pacchioni G., and Di Valentin C. - Transition levels of defect centers in ZnO by hybrid functionals and localized basis set approach, J. Chem. Phys. **133** (2010) 144512.
21. Willander M., Nur O., Sadaf J. R., Qadir M. I., Zaman S., Zainelabdin A., Bano N., and Hussain I. - Luminescence from Zinc Oxide Nanostructures and Polymers and their Hybrid Devices, Materials **3** (2010) 2643–2667.
22. Akazawa H. - Hydrogen induced electric conduction in undoped ZnO and Ga-doped ZnO thin films: Creating native donors via reduction, hydrogen donors, and reactivating extrinsic donors, J. Vac. Sci. Technol. A: Vacuum, Surfaces, and Film **32** (2014) 051511.
23. Gordon R. - Criteria for Choosing Transparent Conductors, MRS Bull. **25** (2000) 52–57.
24. Zhu B. L., Xie M., Wang J., Shi X. W., Wu J., Zeng D. W., and Xie C. S. - Comparative study on effects of $H_2$ flux on structure and properties of Al-doped ZnO films by RF sputtering in Ar+$H_2$ ambient at two substrate temperatures, Ceram. Int. **40** (2014) 12093–12104.
25. Stojilovic N. - Why Can't We See Hydrogen in X-ray Photoelectron Spectroscopy?, J. Chem. Educ. **89** (2012) 1331–1332.

26. Das D., and Mondal P. - Low temperature grown ZnO:Ga films with predominant c-axis orientation in wurtzite structure demonstrating high conductance, transmittance and photoluminescence, RSC Adv. **6** (2016) 6144–6153.
27. Mosquera A. A., Horwat D., Rashkovskiy A., Kovalev A., Miska P., Wainstein D., Albella J. M., and Endrino J. L. - Exciton and core-level electron confinement effects in transparent ZnO thin films, Sci. Rep. **3** (2013) 1714.
28. Han M., Jiang K., Zhang J., Yu W., Li Y., Hu Z., and Chu J. - Structural, electronic band transition and optoelectronic properties of delafossite $CuGa_{1-x}Cr_xO_2$ ($0 \leq x \leq 1$) solid solution films grown by the sol–gel method, J. Mater. Chem. **22** (2012) 18463.
29. Mondal P., and Das D. - Effect of hydrogen in controlling the structural orientation of ZnO:Ga:H as transparent conducting oxide films suitable for applications in stacked layer devices, Phys. Chem. Chem. Phys. **18** (2016) 20450–20458.